Challenge Journal of Structural Mechanics

Research Article

# Design and finite element analysis of a novel auxetic structure

Suleyman Nazif Orhan [a,*], Şeydanur Erden [a]

[a] *Department of Civil Engineering, Erzurum Technical University, 25050 Erzurum, Türkiye*

**ABSTRACT**

In this study, a novel auxetic structure, namely RDN, is presented in two- and three-dimensions. The unit cells are created by modifying the conventional re-entrant structure and the 2D and 3D structures are formed by multiplying these unit cells. Finite element analyses are conducted to study the deformation mechanism of these structures under uniaxial tension, and the mechanical properties of the structures are obtained. Also, a 3D unit cell is modelled with different strut thickness values to examine the effect of the strut thickness on mechanical properties. Numerical models are developed using ANSYS/Static Structural software and linear elastic analyses are performed by applying small displacements to the structures. It is found that the 2D and 3D RDN structures possess a high negative Poisson's ratio but relatively small stiffness compared to the other auxetics. The analyses of the 3D unit cells showed that increasing the strut thickness led to higher stiffness values but reduced auxetic behaviour of the structure.

**ARTICLE INFO**

*Article history:*
Received 24 June 2022
Revised 13 July 2022
Accepted 8 August 2022

*Keywords:*
Negative Poisson's ratio
Auxetic
Finite element analysis
Stiffness

## 1. Introduction

Auxetic structures or materials are characterised by negative Poisson's ratio and contrary to traditional materials, expand due to tensile forces and contract with compressive effects (Fu et al. 2016; Wang et al. 2016). When compared to common materials, auxetic structures have many enhanced and unique mechanical properties such as fracture toughness, energy absorption and synclastic curvature due to their unusual deformation behaviour (Wang et al. 2018; Quan et al. 2020). These features make auxetics attractive for many practical applications such as biomaterials (Kuribayashi et al. 2006; Ali et al. 2014; Kolken et al. 2018; Yao et al. 2021), protective devices (Foster et al. 2018; Krishnan et al. 2021), civil engineering (Assidi and Ganghoffer 2012; Dhanasekar et al. 2016; Zahra and Dhanasekar 2017), sensors (Xu et al. 1999; Ko et al. 2015), aerospace (Liu 2006; Ajaj et al. 2016), and so on.

Although auxetic materials can be found in nature, research into these materials has typically concentrated on manmade structures and started from the pioneering work carried out by Lakes (1987) (Wang et al. 2016; Shepherd et al. 2020). Following Lakes' seminal work, two-dimensional (2D) artificial auxetic structures have experienced remarkable development and the achievements in these 2D structures have provided a great understanding of the nature of the unusual materials. However, with the development of fabrication techniques, three-dimensional (3D) auxetics attracted considerable interest and researchers have triggered a trend to develop more complex 3D models in recent years (Fu et al. 2016; Wang et al. 2018; Gao et al. 2021). Some papers in the literature have examined the mechanical properties of the various existing auxetic structures, while other studies have been carried out to expand the family of auxetic structures and explore potential applications of these structures. Among these studies, Fu et al. (2016) developed a novel 3D re-entrant structure that can achieve a negative Poisson's ratio in two principal orthogonal directions. Lu et al. (2017) proposed two novel auxetic 3D chiral structures based on the 2D cross chiral structure and confirmed that the combined structures have a higher Young's modulus. A new structure named re-entrant chiral auxetic (RCA) was proposed by Alomarah et al. (2019) based on the re-entrant and chiral structures. They compared mechanical properties of this structure with three different auxetic honeycombs and

* *Corresponding author*. Tel.: 444-5-388 ; Fax: +90-442-230-0036 ; E-mail address: s.orhan@erzurum.edu.tr (S. N. Orhan)
ISSN: 2149-8024 / DOI: https://doi.org/10.20528/cjsmec.2022.04.004

stated that the RCA structure offered better energy absorption capacity than the other three auxetics. Qi et al. (2020) replaced the sloped cell wall of a re-entrant hexagonal honeycomb with a double circular arch cell wall and proposed a novel re-entrant circular (REC) structure. The specific energy absorption of the REC structure was found to be much higher than that of the regular re-entrant honeycomb. Su et al. (2020) proposed a unique re-entrant honeycomb structure with reinforcement arches to achieve better structural stiffness while retaining the auxetic behaviour of the structure. Wei et al. (2020) developed a new 3D anti-tetrachiral auxetic and investigated the deformation characteristic of the structure. They found that one of the Poisson's ratios is independent of the geometric parameters. Gao et al. (2021) proposed a class of novel 3D auxetic structures based on the rigid rotating mechanism. They stated that these structures are capable of offering a Poisson's ratio from positive to negative in a wide range along the three principal axes and are suitable for many engineering applications.

As can be seen from the above literature, various researches have been conducted to create new auxetics by modifying the geometries of existing ones. In this paper, a new auxetic lattice structure, namely RDN, was proposed in two- and three-dimensions based on the corresponding re-entrant auxetic topology. The behaviour of these structures under tensile effects was investigated with FEM-based (finite element method) analyses using ANSYS software. From the numerical analyses, stiffness and Poisson's ratio values of these structures were calculated and compared with other auxetic structures. Moreover, the 3D unit cell of the structure was modelled by varying the thickness of the struts between 0.5 and 1.5 mm to investigate the influence of strut thickness on auxetic behaviour. Finally, von Mises stress distributions on the structures were examined.

## 2. Design and Analysis

The RDN structure was designed based on the 2D re-entrant structure geometry. By modifying the 2D re-entrant auxetic, first a 2D unit cell consisting of diagonal and horizontal ligaments was designed, and then a three-dimensional unit cell was modelled (Fig. 1).

The 2D and 3D unit cells were constructed by CAD software SolidWorks 2016 (Dassault Systems, Massachusetts, USA) and by combining the unit cells, two- and three-dimensional structures were obtained as seen in Fig. 2.

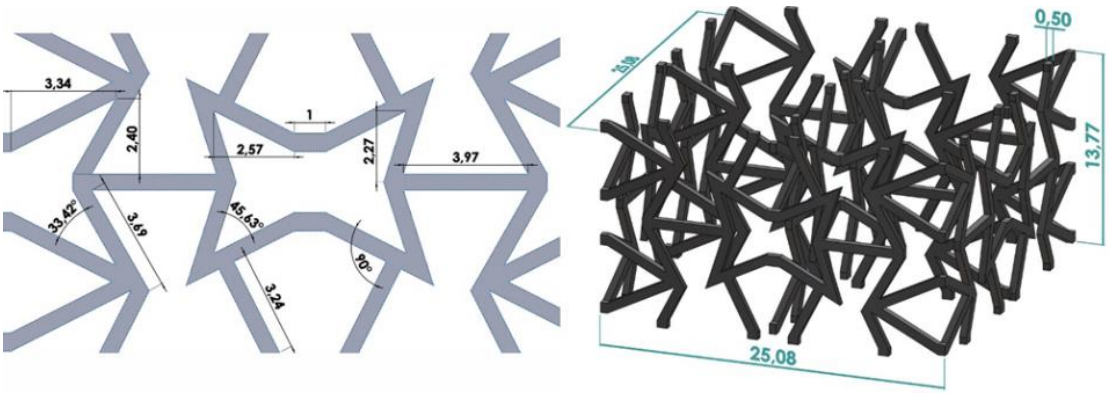


**Fig. 1.** Two- and three-dimensional RDN unit cells (all dimensions in mm).

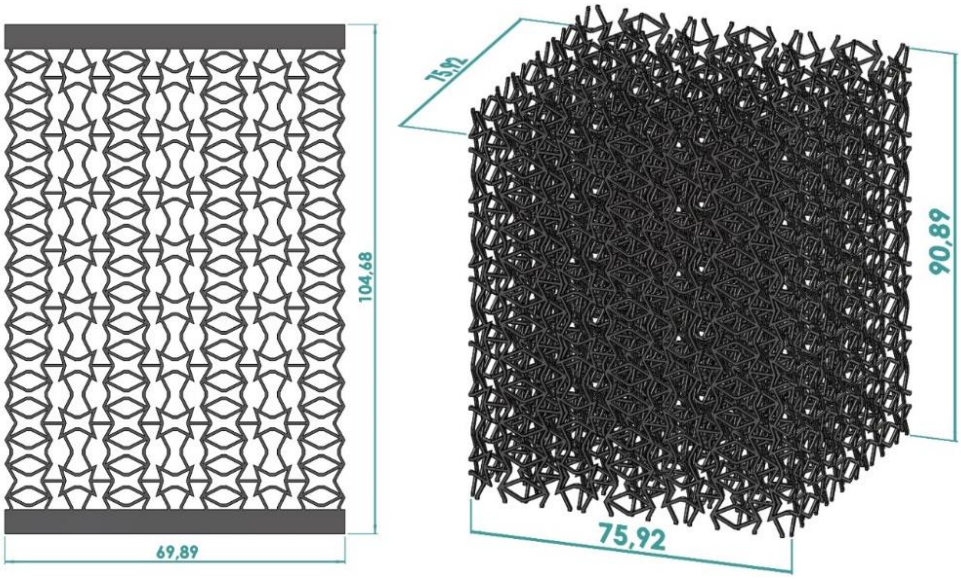


**Fig. 2.** Two- and three-dimensional RDN structures (all dimensions in mm).

In modelling these structures, the dimensions of our previously examined auxetic structures (Orhan and Erden 2022) were taken into account. Thus, the mechanical properties were intended to be comparable. Finite element analyses were conducted to examine the behaviour of these structures under displacements as uniaxial tension and the stiffness and Poisson's ratio of the structures were determined. Besides, the 3D unit cells were modelled with four different strut thickness values (0.5, 1, 1.2 and 1.5 mm) to explore the effect of strut thickness on the auxeticity of the RDN structure.

The numerical simulations of the structures were performed using the Static Structural analysis module of the ANSYS Workbench (v20.R1) (ANSYS Inc., PA, USA) software. To determine the mesh element size and the boundary conditions, the results of the validation and mesh convergence study we had previously performed and presented were taken into account. In our previous study (Orhan and Erden 2022), we modelled and analysed the re-entrant structures that were investigated numerically and experimentally by Wang et al. (2016) and compared the results to validate our models. Detailed information about these analyses was given in our previous paper. In line with the results obtained from the validation study, the boundary conditions applied in the analyses are shown in Fig. 3. All structures were fixed from one side and a constant displacement was applied to the other side. Two platens of thickness 5 mm, were placed to the top and bottom sides of the 3D structure and platens were fixed on the structure employing "bonded" contact. In the 3D unit cells, fixation and loading were made directly on the surface of the struts, and no platens were used. Displacement values were taken as 1/1000 of the structures' heights $(\varepsilon_y \leq 0.001)$ to conduct analyses in the linear elastic region. In the analyses, all structures were meshed with hexahedron (hex20) elements and the selected mesh size was of 0.67 mm following our previous mesh convergence study. The "structural steel" from the ANSYS material library was defined as material for all RDN structures in the analysis (Table 1).

Considering the points seen in Fig. 3 and using Eqs. (1) and (2) given below, the Poisson's ratio ($\nu_{yx}$) of each RDN auxetic was determined. Also, the force values corresponding to the applied displacements were obtained for each structure and force-displacement curves were created. The stiffness of the auxetics was derived from the slope of these curves.

**Table 1.** Material properties used in numerical analysis.

| Material | Density | Young's modulus | Poisson's ratio | Tensile yield strength | Tensile ultimate strength |
|---|---|---|---|---|---|
| Structural steel | 7.85 gr/cm³ | 200 GPa | 0.3 | 0.25 GPa | 0.46 GPa |

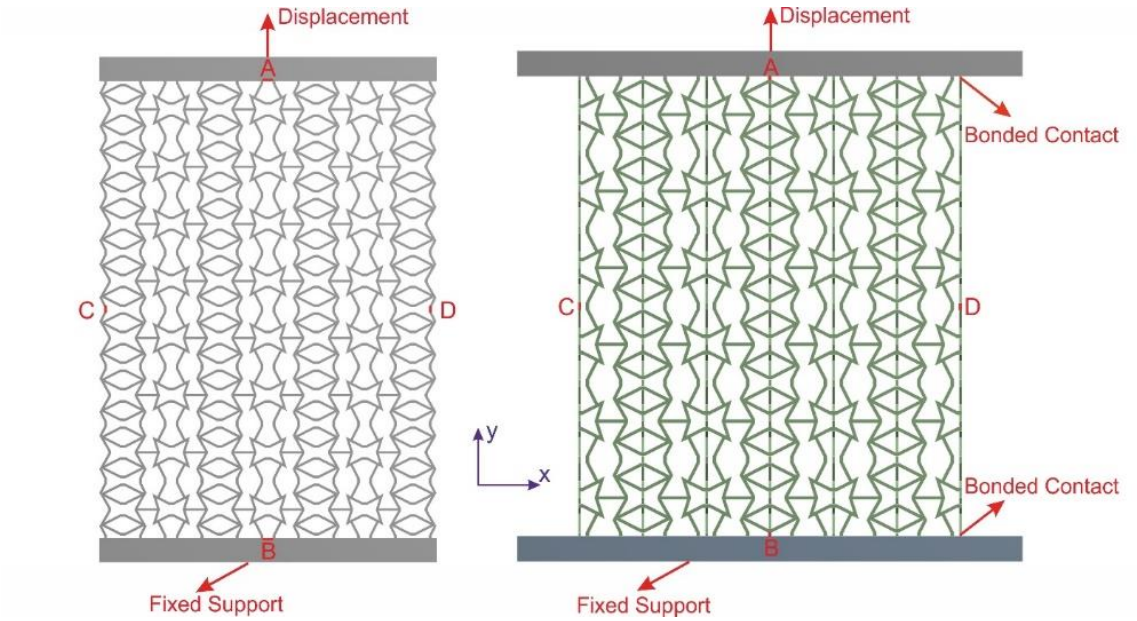


**Fig. 3.** Boundary conditions used in FEM analysis.

$$\varepsilon_x = \frac{\Delta L_x}{L_x} \quad , \quad \varepsilon_y = \frac{\Delta L_y}{L_y} \tag{1}$$

$$\nu_{yx} = -\frac{\varepsilon_x}{\varepsilon_y} \tag{2}$$

where, $\varepsilon_y$ is the strain calculated in the longitudinal direction, $\varepsilon_x$ is the strain calculated in the lateral direction, $L_x$ and $L_y$ are the original distances between points C-D and A-B, respectively, and $\Delta L_x$ and $\Delta L_y$ are the change in distances between these points after deformation.

## 3. Results and Discussion

The force-displacement curves generated from the analyses of the two- and three-dimensional RDN structures are illustrated in Fig. 4 and the stiffness and Poisson's ratio values of the structures are given in Table 2.

From these results, it is seen that the 2D and 3D RDN structures showed auxetic behaviour as desired and had a high negative Poisson's ratio. When these results were compared with the previously examined re-entrant, lozenge grid, arrowhead and elliptic hole structures (Orhan and Erden 2022), the stiffness and Poisson's ratio values of the 2D RDN were found to be larger than the values obtained from the re-entrant and lozenge grid structures. In three dimensions, it is determined that the Poisson's ratio of the RDN structure was larger than those of the re-entrant and lozenge grid structures, and the stiffness value was smaller than that of the other four auxetics.

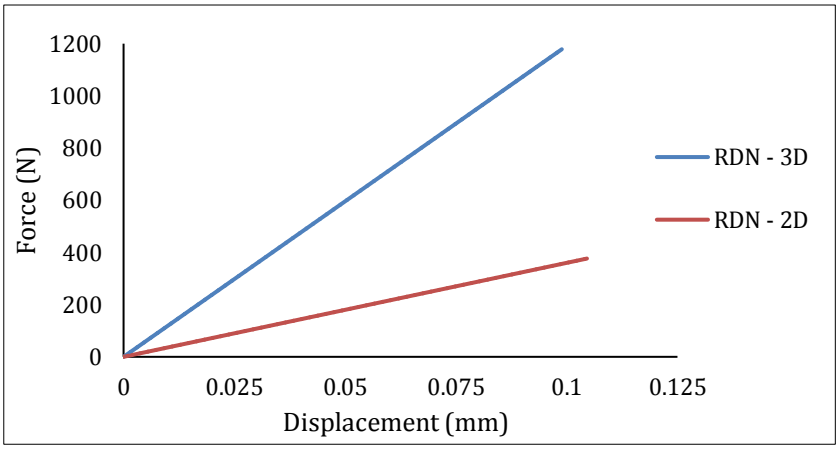


**Fig. 4.** Force-displacement curves of the RDN structures.

**Table 2.** Mechanical properties of the RDN structures obtained from the analyses.

| Auxetic | Stiffness (N/mm) | | Poisson's Ratio | |
|---|---|---|---|---|
| | 2D | 3D | 2D | 3D |
| RDN | 3601 | 11916 | -0.704 | -0.806 |

When the von Mises stresses at the 2D and 3D RDN auxetics were examined, it was seen that the maximum von Mises stresses occurred at the corner points where the longitudinal struts are connected to the horizontal elements (Fig. 5). The highest von Mises stresses of 259.1 MPa and 212.8 MPa were found at the 2D and 3D structures, respectively. In order to reduce the stress concentration, the edges can be substituted by curves.

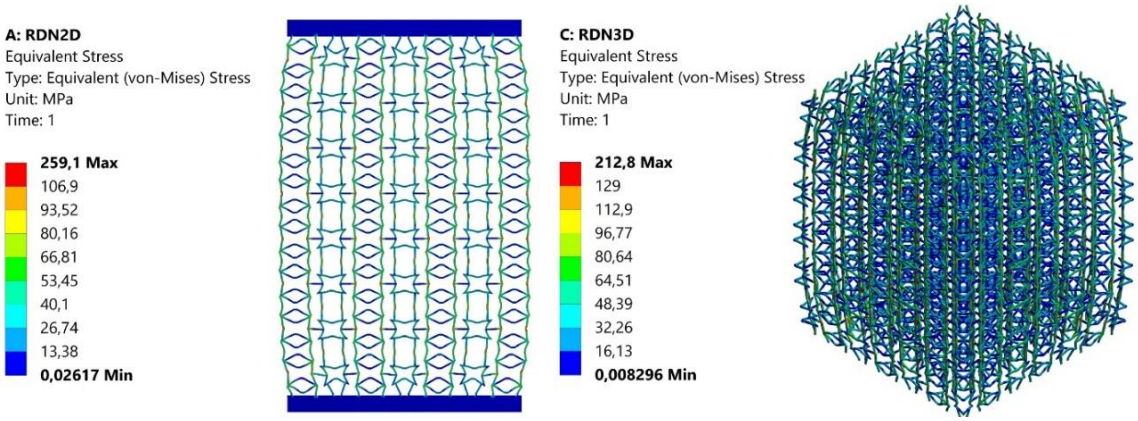


**Fig. 5.** Maximum von Mises stresses at the RDN structures.

The force-displacement curves obtained from the analyses of the 3D unit cells modelled with different strut thickness values are shown in Fig. 6. The Poisson's ratio, relative density and stiffness values of these unit cells are also given in Table 3. It is found that the Poisson's ratio decreases from -0.793 to -0.663 and stiffness increases from 22876 N/mm to 60874 N/mm with an increase of thickness from 0.5 mm to 1.5 mm. Although in a study conducted by Meena et al. (2019), it was stated that the thickness had no discernible effect on the auxetic behaviour of the structure, our results were consistent with other studies where it was indicated that the Poisson's ratio of the auxetic structure decreases with increase of strut thickness (Lee et al. 1996; Schwerdtfeger et al. 2012; Ren et al. 2015). The Poisson's ratio and stiffness values versus strut thickness are plotted in Fig. 7.

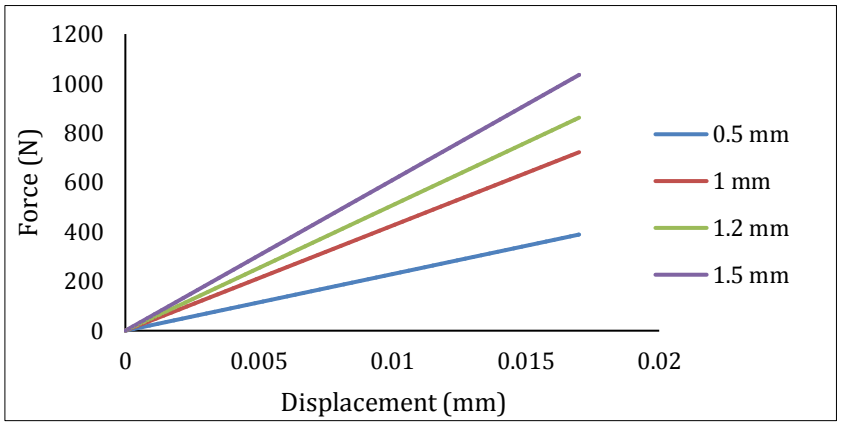


**Fig. 6.** Force-displacement curves of the 3D RDN unit cells.

**Table 3.** The effect of strut thickness on the mechanical properties of the unit cell.

| Strut thickness (mm) | Poisson's ratio | Stiffness (N/mm) | Relative density (%) |
|---|---|---|---|
| 0.5 | -0.793 | 22876 | 0.0321 |
| 1.0 | -0.721 | 42475 | 0.0508 |
| 1.2 | -0.688 | 50694 | 0.0616 |
| 1.5 | -0.663 | 60874 | 0.0716 |

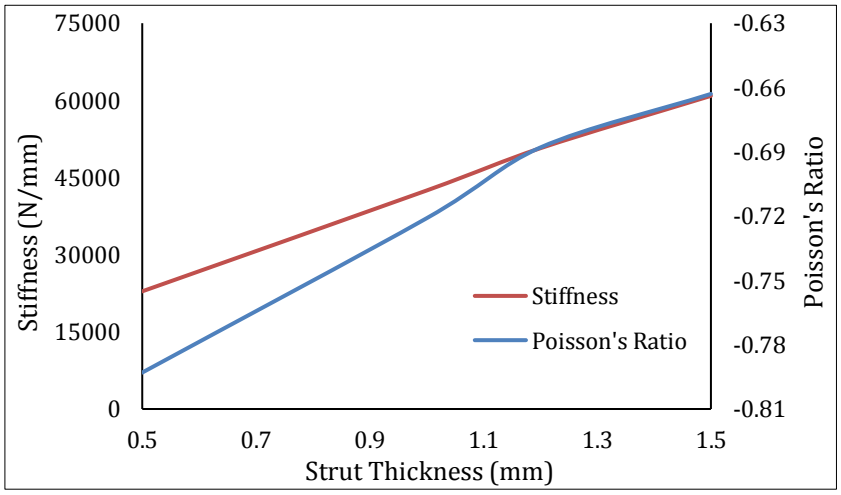


**Fig. 7.** Poisson's ratio and stiffness change with strut thickness.

Fig. 8 shows the stress distribution along the 3D unit cells with different strut thicknesses. The maximum von Mises stress was obtained as 347 MPa at the unit cell with 0.5 mm strut thickness. As the strut thickness and the relative density of the unit cell increased, the stress values gradually decreased. Hence, the largest stress was determined as 305.5 MPa for the unit cell with 1.5 mm strut thickness. The percentage change of the maximum von Mises stress with respect to the change of strut thickness is shown in the Table 4.

**Table 4.** Change of the maximum von Mises stress with increasing strut thickness.

| | Strut thickness (mm) | | | |
|---|---|---|---|---|
| | 0.5 | 1 | 1.2 | 1.5 |
| Percentage increase of the strut thickness (%) | | 100 | 140 | 200 |
| Maximum von Mises stress (MPa) | 347 | 333.3 | 321.6 | 305.5 |
| Percentage decrease of the maximum von Mises stress (%) | | 3.95 | 7.32 | 11.96 |

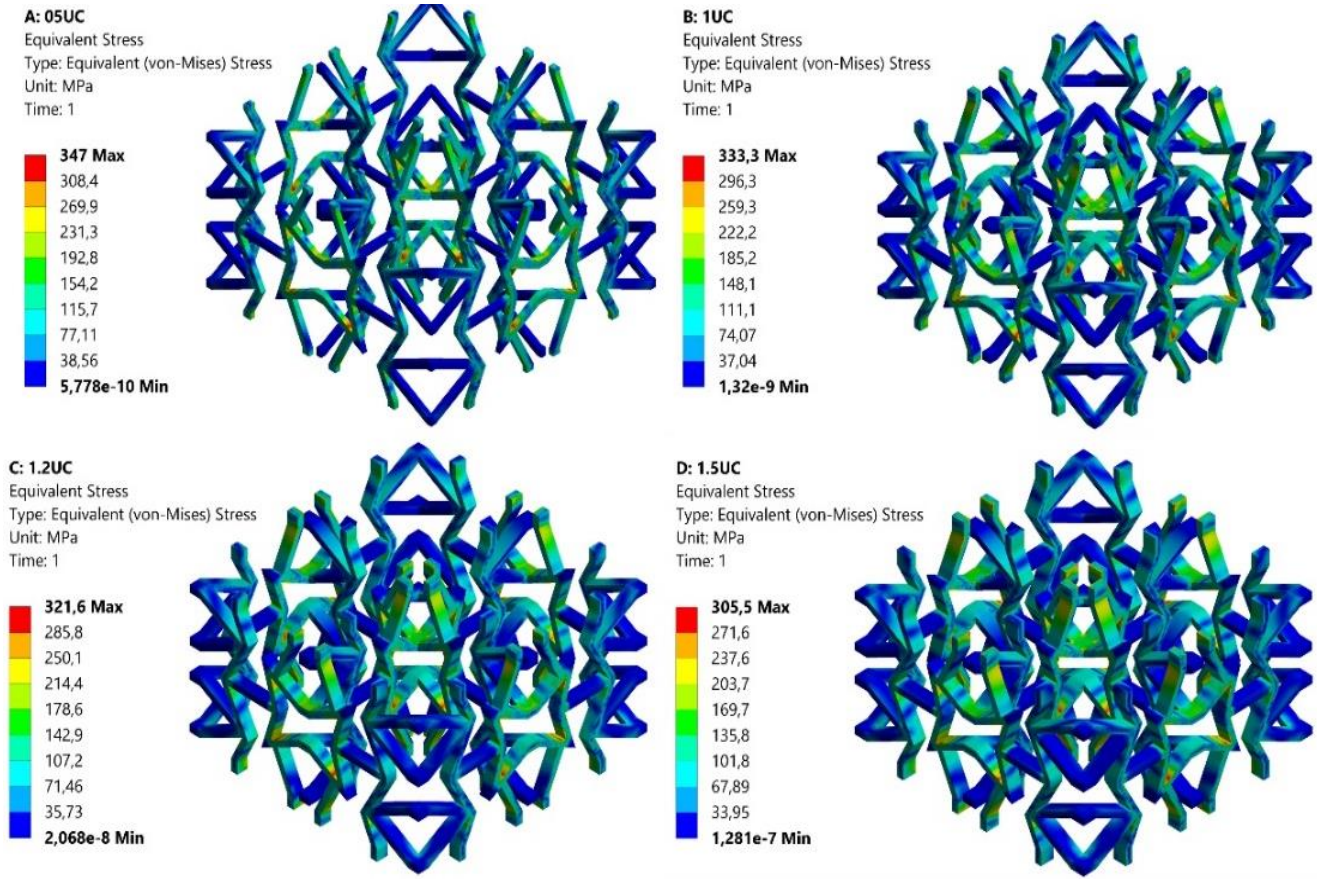


**Fig. 8.** Maximum von Mises stress distributions at the 3D unit cells.

## 4. Conclusions

In this present work, a new auxetic lattice structure was proposed in two- and three-dimensions. The design of this structure was carried out by modifying the conventional re-entrant auxetic. Finite element analyses were conducted under axial extension to determine the mechanical properties and the deformation characteristics of these structures. The analyses showed that the structures are capable of offering auxetic behaviour and a high negative Poisson's ratio. It was found that the Poisson's ratio of the 3D RDN auxetic was greater than the lozenge grid and re-entrant structures but the stiffness of the structure was lower when compared with the re-entrant, lozenge grid, arrowhead and elliptic hole structures. However, this design is the first step for the RDN structure. Considering the stress distribution in the structure, the unit cell modifications and shape optimisation can be performed, and the mechanical performance of the structures can be enhanced. In addition, analyses can be carried out under both quasi-static and dynamic compression loads to determine other mechanical properties of the structure, like compressive and buckling strength. Furthermore, experimental investigation of the presented structures could be performed and the possible application of the structure in different fields such as biomedicine or civil engineering could be determined in future works.

## Acknowledgements

None declared.

## Funding

The authors received no financial support for the research, authorship, and/or publication of this manuscript.

## Conflict of Interest

The authors declared no potential conflicts of interest with respect to the research, authorship, and/or publication of this manuscript.

## References

Ajaj RM, Beaverstock CS, Friswell MI (2016). Morphing aircraft: The need for a new design philosophy. *Aerospace Science and Technology*, 49, 154-166.

Ali MN, Busfield JJC, Rehman IU (2014). Auxetic oesophageal stents: structure and mechanical properties. *Journal of Materials Science-Materials in Medicine*, 25(2), 527-553.

Alomarah A, Ruan D, Masood S, Gao Z (2019). Compressive properties of a novel additively manufactured 3D auxetic structure. *Smart Materials and Structures*, 28(8), 085019.

Assidi M, Ganghoffer JF (2012). Composites with auxetic inclusions showing both an auxetic behavior and enhancement of their mechanical properties. *Composite Structures*, 94(8), 2373-2382.

Dhanasekar M, Thambiratnam DP, Chan THT, Noor-E-Khuda S, Zahra T (2016). Modelling of masonry walls rendered with auxetic foam layers against vehicular impacts. *Brick and Block Masonry: Trends, Innovations and Challenges*, Padova, Italy, 977-983.

Foster L, Peketi P, Allen T, Senior T, Duncan O, Alderson A (2018). Application of auxeticfoam in sports helmets. *Applied Sciences-Basel*, 8(3), 354.

Fu MH, Chen Y, Zhang WZ, Zheng BB (2016). Experimental and numerical analysis of a novel three-dimensional auxetic metamaterial. *Physica Status Solidi B-Basic Solid State Physics*, 253(8), 1565-1575.

Gao Y, Wei XY, Han XK, Zhou ZG, Xiong J (2021). Novel 3D auxetic lattice structures developed based on the rotating rigid mechanism. *International Journal of Solids and Structures*, 233, 111232.

Ko J, Bhullar S, Cho YY, Lee PC, Jun MBG (2015). Design and fabrication of auxetic stretchable force sensor for hand rehabilitation. *Smart Materials and Structures*, 24(7), 075027.

Kolken HMA, Janbaz S, Leeflang SMA, Lietaert K, Weinans HH, Zadpoor AA (2018). Rationally designed meta-implants: a combination of auxetic and conventional meta-biomaterials. *Materials Horizons*, 5(1), 28-35.

Krishnan BR, Biswas AN, Kumar KVA, Sreekanth PSR (2021). Auxetic structure metamaterial for crash safety of sports helmet. *Materials Today: Proceedings*, 56(3), 1043-1049.

Kuribayashi K, Tsuchiya K, You Z, Tomus D, Umemoto M, Ito T, Sasaki M (2006). Self-deployable origami stent grafts as a biomedical application of Ni-rich TiNi shape memory alloy foil. *Materials Science and Engineering a-Structural Materials Properties Microstructure and Processing*, 419(1-2), 131-137.

Lakes R (1987). Foam structures with a negative Poisson's ratio. *Science*, 235(4792), 1038-1040.

Lee J, Choi JB, Choi K (1996). Application of homogenization FEM analysis to regular and re-entrant honeycomb structures. *Journal of Materials Science*, 31, 4105- 4110.

Liu Q (2006). Literature review: Materials with negative Poisson's ratios and potential applications to aerospace and defence. *Defence Science and Technology Organisation*, Victoria, Australia.

Lu Z, Wang Q, Li X, Yang Z (2017). Elastic properties of two novel auxetic 3D cellular structures. *International Journal of Solids and Structures*, 124, 46-56.

Meena K, Calius EP, Singamneni S (2019). An enhanced square-grid structure for additive manufacturing and improved auxetic responses. *International Journal of Mechanics and Materials in Design*, 15, 413-426.

Orhan SN, Erden Ş (2022). Numerical investigation of the mechanical properties of 2D and 3D auxetic structures. *Smart Materials and Structures*, 31(6), 065011.

Qi C, Jiang F, Remennikov A, Pei LZ, Liu J, Wang JS, Liao XW, Yang S (2020). Quasi-static crushing behavior of novel re-entrant circular auxetic honeycombs. *Composites Part B: Engineering*, 197, 108117.

Quan C, Han B, Hou ZH, Zhang Q, Tian XY, Lu TJ (2020). 3d printed continuous fiber reinforced composite auxetic honeycomb structures. *Composites Part B-Engineering*, 187, 107858.

Ren X, Shen J, Ghaedizadeh A, Tian H, Xie YM (2015). Experiments and parametric studies on 3D metallic auxetic matematerials with tuneable mechanical properties. *Smart Materials and Structures*, 24(9), 095016.

Schwerdtfeger J, Schury F, Stingl M, Wein F, Singer RF, Körner C (2012). Mechanical characterisation of a periodic auxetic structure produced by SEBM. *Physica Status Solidi B-Basic Solid State Physics*, 249(7), 1347-1352.

Shepherd T, Winwood K, Venkatraman P, Alderson A, Allen T (2020). Validation of a finite element modeling process for auxetic structures under impact. *Physica Status Solidi B-Basic Solid State Physics*, 257(10).

Su Y, Wu X, Shi J (2020). A novel 3D printable multimaterial auxetic metamaterial with reinforced structure: Improved stiffness and retained auxetic behavior. *Mechanics of Advanced Materials and Structures*, 29(3), 408-418.

Wang XT, Li XW, Ma L (2016). Interlocking assembled 3D auxetic cellular structures. *Materials & Design*, 99, 467-476.

Wang XT, Wang B, Wen ZH, Ma L (2018). Fabrication and mechanical properties of CFRP composite three-dimensional double-arrow-head auxetic structures. *Composites Science and Technology*, 164, 92-102.

Wei YL, Yang QS, Liu X, Tao R (2020). A novel 3D anti-tetrachiral structure with negative Poisson's ratio. *Smart Materials and Structures*, 29(8), 085003.

Xu B, Arias F, Brittain ST, Zhao XM, Grzybowski B, Torquato S, Whitesides GM (1999). Making negative Poisson's ratio microstructures by soft lithography. *Advanced Materials*, 11(14), 1186-1189.

Yao Y, Yuan H, Huang HW, Liu JL, Wang LZ, Fan YB (2021). Biomechanical design and analysis of auxetic pedicle screw to resist loosening. *Computers in Biology and Medicine*, 133, 104386.

Zahra T, Dhanasekar M (2017). Characterisation of cementitious polymer mortar - Auxetic foam composites. *Construction and Building Materials*, 147, 143-159.